# Modeling Optical Sensors Based on Carbon Nanotubes

(*Invited*)

Mahdi Pourfath and Siegfried Selberherr*

Institute for Microelectronics, TU Wien, A-1040 Vienna, Austria
E-mail: {pourfath|selberherr}@iue.tuwien.ac.at

*Abstract*- **Graphite related materials such as fullerenes, carbon nanotubes, and graphene nanoribbons have been extensively studied in recent years due to their exceptional electronic, optoelectronic and mechanical properties. The direct band gap and the tuneability of the relatively narrow band gap with the tube diameter or ribbon's width render them as suitable candidates for optoelectronic devices, especially for infrared applications. The performances of nanotube and nanoribbon based infra-red photo detectors are analyzed, using the non-equilibrium Green's function formalism.**

*Index Terms*- **carbon nanotube, graphene nanoribbon, photo detector, quantum transport, non-equilibrium Green's function formalism,**

## I. INTRODUCTION

Graphene, a one-atomic carbon sheet with a honeycomb structure, has attracted significant attention due to its unique physical properties [1]. This material shows an extraordinarily high carrier mobility of more than $2\times10^5$ $cm^2/V.s$ [2] and is considered to be a major candidate for future high speed transistor materials. One of the most interesting properties of electrons in graphene is the drastic change of the conductivity with the confinement of the electrons. Structures based on graphene with this behavior are *carbon nanotubes* (CNTs) and *graphene nanoribbons* (GNRs) with, respectively, periodic and zero boundary conditions for the transverse electron wave vector. A CNT can be viewed as a rolled-up sheet of graphene with a diameter of a few nanometers. The way the graphene sheet is wrapped is represented by a pair of indices $(n,m)$ called the chiral vector. The electronic properties of a CNT exhibit a dependence on the chiral vector. CNT based devices have been the subject of intensive research for the last decade [3].

Recently, graphene sheets have been patterned into narrow nanoribbons [4]. These GNRs have attracted much interest as they are recognized as promising building blocks for nanoelectronic devices [5]. The electronic properties of GNRs exhibit a dependence on the ribbon direction and width. In comparison with CNTs, there are some key potential advantages in designing and constructing device architectures based on GNRs [6]. First, all the junctions between GNRs of different width and directionality have a perfect atomic interface, a feature which is difficult to achieve for interfacing CNTs of different diameter and chirality. Second, it is generally difficult to find a robust method to make a contact with a molecular device unit, because there exists usually a large resistance between the metal electrodes and the molecules due to a very small contact area. This difficulty may be circumvented by using GNRs, because the GNR based devices can be connected to the outside circuits exclusively via semi-metallic GNRs.

The direct band gap and the tuneability of the band gap with the tube diameter or ribbon's width render CNTs and GNRs as suitable candidates for optoelectronic devices, especially for infra-red applications [7, 8], in particular, due to the relatively narrow band gap [8, 9]. To explore the physics of such devices quantum mechanical simulations have been performed, employing the non-equilibrium Green's function formalism (NEGF). This method has been successfully used to investigate the characteristics of CNT-FETs [10]. We utilized the NEGF method along with a tight-binding model to study quantum transport in CNT and GNR based infrared (IR) photo detectors.

## II. NON-EQUILIBRIUM GREEN'S FUNCTION FORMALISM

The NEGF formalism initiated by Schwinger, Kadanoff, and Baym [11] allows one to study the time evolution of a many-particle quantum system. The many-particle information about the system is cast into self-energies which are part of the equations of motion for the Green's functions. A perturbation expansion of the Green's functions is the key to approximate the self-energies. Green's functions enable a powerful technique to evaluate the properties of a many-body system both in thermodynamic equilibrium and non-equilibrium situations. Four types of Green's functions are defined as the non-equilibrium statistical ensemble averages of the single particle correlation operator [11]. The greater Green's function $G^{>}$ and the lesser Green's function $G^{<}$ deal with the statistics of carriers. The retarded Green's function $G^{\mathrm{R}}$ and the advanced Green's function $G^{\mathrm{A}}$ describe the dynamics of carriers. Under steady-state condition the equation of motion for the Green's functions can be written as [12]:

$$\left[E-\widehat{H}_0\right]G^{\mathrm{R,A}}(1,2) - \int d3\,\Sigma^{\mathrm{R,A}}(1,3)\mathrm{G}^{\mathrm{R,A}}(3,2) = \delta_{1,2} \tag{1}$$

$$G^{\lessgtr}(1,2) = \int d3 \int d4\; G^{\mathrm{R}}(1,3)\Sigma^{\lessgtr}(3,4)\, G^{\mathrm{A}}(4,2) \tag{2}$$

The abbreviation $1 \equiv (\boldsymbol{r}_1, t_1)$ is used. $\widehat{H}_0$ is the single-particle Hamiltonian operator and $\Sigma^{\mathrm{R}}$, $\Sigma^{<}$, and $\Sigma^{>}$ are the retarded, lesser, and greater self-energies, respectively.

## III. IMPLEMENTATION

This section deals with the implementation of the outlined NEGF formalism for the numerical analysis of CNT and GNR based devices. A tight-binding Hamiltonian is used to describe transport phenomena in such devices. The self-energy due to electron-photon interactions is studied next.

### *A. Tight-Binding Hamiltonian*

In Graphene three $\sigma$ bonds hybridize in an $sp^2$ configuration, whereas the other $2p_z$ orbital, which is perpendicular to the graphene layer, forms $\pi$ covalent bonds. We use a tight-binding Hamiltonian of the $\pi$ band electron to describe the electronic properties of GNRs and CNTs:

$$\widehat{H}_0 = t\sum_{\langle i,j\rangle} \hat{a}_i^{\dagger}\hat{a}_j \tag{3}$$

The summation is restricted between the pairs of the nearest-neighbor carbon atoms, $t = -2.7$ eV is the hopping parameter, and the onsite potential is assumed to be zero.

### *B. Electron-Photon Self-Energies*

The Hamiltonian of the electron-photon interaction can be written as:

$$\widehat{H}_{\omega} = \sum_{\langle i,j\rangle} \frac{\mathrm{q}}{m_0}\boldsymbol{A}\cdot\langle i|\hat{\boldsymbol{p}}|j\rangle \tag{4}$$

$\hat{\boldsymbol{p}}$ is the momentum operator and $\boldsymbol{A}$ is the vector potential. It can be shown that the second quantized vector potential, $\boldsymbol{A}$, is given by

$$\boldsymbol{A} = \hat{\boldsymbol{a}}\sqrt{\frac{\hbar I_{\omega}}{2N_{\omega}c\varepsilon\omega}}\left(\hat{b}e^{-i\omega t} + \hat{b}^{\dagger}e^{i\omega t}\right) \tag{5}$$

The direction of $\boldsymbol{A}$ is determined by the polarization of the field, which is denoted by $\hat{\boldsymbol{a}}$. $I_{\omega}$ is the flux of photons with frequency $\omega$, and $N_{\omega}$ is the photon population number. By using the operator relation $\hat{\boldsymbol{p}} = im_0\hbar^{-1}[\widehat{H}, \hat{\boldsymbol{r}}]$ one obtains [13]:

$$\widehat{H}_{\omega} = \sum_{\langle i,j\rangle} M_{ij}\left(\hat{b}e^{-i\omega t} + \hat{b}^{\dagger}e^{i\omega t}\right)\hat{a}_i^{\dagger}\hat{a}_j \tag{6}$$

$$M_{i,j} = \left(z_j - z_i\right)\frac{i\mathrm{q}}{\hbar}\sqrt{\frac{\hbar I_{\omega}}{2N\omega c\varepsilon}}\langle i|\widehat{H}_0|j\rangle \tag{7}$$

Here $z_i$ denotes the position of the carbon atom at site $i$. The incident light is assumed to be monochromatic with polarization along the CNT axis. We employed the lowest order self-energy of the electron-photon interaction based on the self-consistent Born approximation [13]:

$$\Sigma^{<}_{i,j}(E) = \sum_{p,q} M_{i,p} M_{q,j} [N_\omega G_{p,q}(E - \hbar\omega) + (N_\omega + 1) G_{p,q}(E + \hbar\omega)] \quad (8)$$

The first term corresponds to the excitation of an electron by the absorption of a photon and the second term corresponds to the emission of a photon by de-excitation of an electron.

## IV. SIMULATION RESULTS

In this section the non-locality of the electron-photon interaction will be studied first. Photo absorption in CNTs and GNRs is discussed next.

### *A. Non-Locality of Electron-Photon Interaction*

When scattering via a self-energy is introduced, the determination of the Green's function requires inversion of a matrix of huge rank. To reduce the computational cost, the *local scattering approximation* is frequently used [14], where the scattering self-energy terms are diagonal in their coordinate representation. This allows utilizing a recursive algorithm for computing the Green's functions [14]. The local approximation is well justified for electron-phonon scattering caused by deformation potential interaction [15]. However, this approximation is not justified for describing properly the electron-photon interaction. For the given structure the calculated photo current is depicted in Fig.1. The results are given as a function of the number of included off-diagonal elements of the retarded self-energy, which includes the effects of electron-photon interaction. With only the diagonal elements of the self-energy (local scattering approximation) the calculated current is only four percent of its value as in case of full matrix consideration.

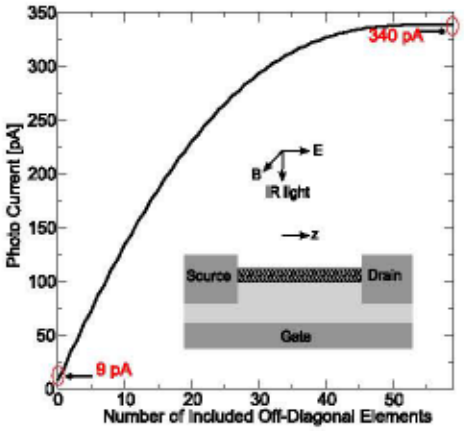


Fig.1 The calculated photo current as a function of the included off-diagonal elements of the self-energy. The full matrix size is 60 × 60. The inset of the figure shows the sketch of the simulated device. The length of the device is approximately 13nm.

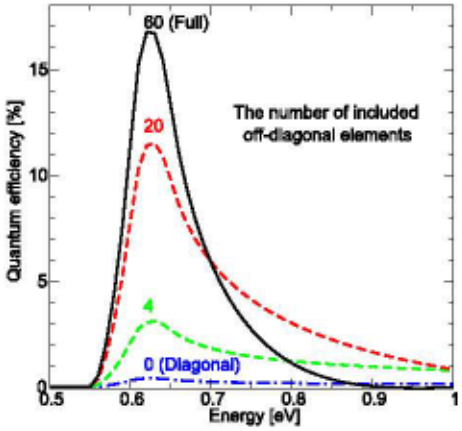


Fig.2 The quantum efficiency of the CNT as a function of the incident photon energy. The number of included off-diagonal elements of the self-energy has a strong influence on the calculated quantum efficiency.

### *B. Photo Absorption in CNTs*

To investigate GNR photo detectors we study the quantum efficiency which is defined as:

$$\alpha = \frac{I_{\mathrm{Ph}}/\mathrm{q}}{P_{\mathrm{Op}}/\hbar\omega} \quad (9)$$

$I_{\mathrm{Ph}}$ is the photo current and $P_{\mathrm{Op}}$ is the incident optical power. This quantity corresponds in fact to the energy conversion efficiency of a photo detector. Fig.2 shows the quantum efficiency of the CNT as a function of the incident photon

energy. The efficiency is maximized, when the photon energy matches the band gap of the CNT. However, at this energy the proper inclusion of off-diagonal elements becomes more important. This can be understood by considering the fact that at that peak the carrier energy is close to the conduction and valence band energy, where it has a longer wave-length. This result is in agreement with experimental data, where the maximum quantum efficiency is estimated to be between 10-20 percent [8].

### *C. Photo Absorption in GNRs*

Fig.3 shows the density of states of a 12 −armchair GNR for the first three subbands. Van-hove singularities in the density of states result in large photon-assisted transitions from the valence band to the conduction band. Some of the most important transitions are marked. Fig.4 shows the calculated quantum efficiency of the investigated device as a function of the incident photon energy. The efficiency is maximized, when the photon energy matches the band gap of the GNR. The maximum quantum efficiency ranges from 9% to 11% and is fairly independent of the band gap [16]. Due to the periodic boundary conditions, the subbands of CNTs appear as double degenerate. However, in GNRs this symmetry is removed and subbands are no longer degenerate. As a result the current capacity in GNRs is roughly half of that of their CNT counterparts. It is, therefore, reasonable to expect a maximum quantum efficiency of 10% in GNR devices.

## VI. CONCLUSION

We have presented a study of optoelectronic properties of CNT and GNR based devices employing the NEGF method. The results are in good agreement with experimental data. The results show that the local scattering approximation which is widely used in quantum transport simulations, fails to predict the behavior of devices, where electron-photon interaction is present. For accurate simulations a non-local self-energy must be taken into account.

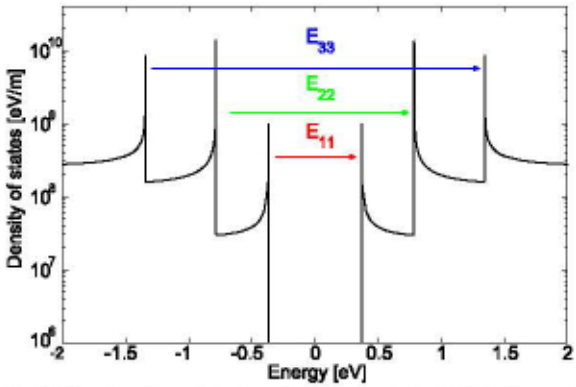


Fig.3 The density of states of a 12-armchair GNR. Some of the most important transitions are marked: $E_{i,j}$ denotes a transition from the *i-th* valence band to the *j-th* conduction band.

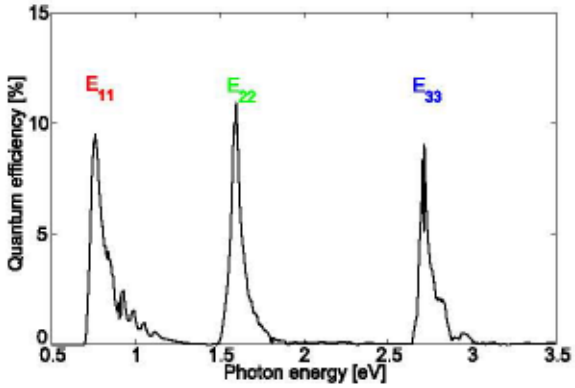


Fig.4 The calculated quantum efficiency as a function of the incident photon energy.

## REFERENCES

[1] J. Appenzeller, *Proc. IEEE* **96**, 201 (2008).
[2] X. Du *et al.*, *Nature Nanotech.* **3**, 491 (2008).
[3] P. Avouris *et al.*, *Nature Nanotech.* **2**, 605 (2007).
[4] C. Berger *et al.*, *Science* **312**, 1191 (2006).
[5] M. Freitag, *Nature Nanotech.* **3**, 455 (2008).
[6] Q. Yan *et al.*, *Nano Lett.* **7**, 1469 (2007).
[7] M. Freitag *et al.*, *Phys. Rev. Lett.* **93**, 076803 (2004).
[8] M. Freitag *et al.*, *Nano Lett.* **3**, 1067 (2003).
[9] S. Lu *et al.*, *Nanotechnology* **17**, 1843 (2006).
[10] M. Pourfath *et al.*, *Nanotech.* **18**, 424036 (2007).
[11] G. D. Mahan, *Many-Particle Physics, Physics of Solids and Liquids*, 2nd ed., Plenum Press (1990).
[12] S. Datta, *Electronic Transport in Mesoscopic Systems*, Cambridge University Press (1995).
[13] L. E. Henrickson, *J. Appl. Phys.* **91**, 6273 (2002).
[14] R. Lake *et al.*, *J. Appl. Phys.* **81**, 7845 (1997).
[15] S. O. Koswatta *et al.*, *IEEE Trans. Electron Devices* **54**, 2339 (2007).
[16] D. A. Stewart *et al.*, *Phys. Rev. Lett.*, **93**, 107401 (2004).